# Electrical conductivity of $In_2O_3$ and $Ga_2O_3$ after low temperature ion irradiation; implications for intrinsic defect formation and charge neutrality level

L. Vines[1],* C. Bhoodoo[1], H. von Wenckstern[2], and M. Grundmann[2]

[1] *University of Oslo, Department of Physics/Centre for Materials Science and Nanotechnology, P.O. Box 1048 Blindern, N-0316 Oslo, Norway and*

[2] *Institut für Experimentelle Physik II, Fakultät für Physik und Geowissenschaften, Universität Leipzig, Linnestraße 5, 04103 Leipzig, Germany*

(Dated: November 25, 2017)

## Abstract

The evolution of sheet resistance of n-type $In_2O_3$ and $Ga_2O_3$ exposed to bombardment with MeV $^{12}C$ and $^{28}Si$ ions at 35 K is studied in situ. While the sheet resistance of $Ga_2O_3$ increased by more than 8 orders of magnitude as a result of ion irradiation, $In_2O_3$ showed a more complex defect evolution and became more conductive when irradiated at the highest doses. Heating up to room temperature reduced the sheet resistivity somewhat, but $Ga_2O_3$ remained highly resistive, while $In_2O_3$ showed a lower resistance than as deposited samples. Thermal admittance spectroscopy and deep level transient spectroscopy did not reveal new defect levels for irradiation up to $2 \times 10^{12}$ $cm^{-2}$. A model where larger defect complexes preferentially produce donor like defects in $In_2O_3$ is proposed, and may reveal a microscopic view of a charge neutrality level within the conduction band, as previously proposed.

PACS numbers:

*Electronic address: Lasse.Vines@fys.uio.no

## I. INTRODUCTION

The semiconducting oxides (SO) gallium oxide ($Ga_2O_3$), indium oxide ($In_2O_3$) and zinc oxide (ZnO) show n-type conductivity and have a wide and direct band gap with interesting potential applications as transparent conductive oxides for display and energy application[1] [2], UV detectors and power electronics[3] [4]. However, in order to realize devices with optimized performance, the bulk as well as the surface properties of the oxide layers must be controllable and adjustable, where intrinsic defects play a key role.

The so called branch point or Fermi level stabilization energy has proved to be a highly useful material parameter for a general understanding of dielectric or electric properties [5, 6], the formation of intrinsic defects [7, 8], the formation of Schottky barriers [9, 10] or the position of transition metal [10] or the hydrogen level [11] in semiconductor and the band alignment at heterointerfaces [9][12–17]. In most semiconductors this branch point energy or charge neutrality level (CNL) is located close to the middle of the band gap, where e.g. ion irradiation would preferentially produce donor like defects in p-type material, whereas acceptor defects would previal in n-type material. Thus, CNL can explain e.g. the ion irradiation induced electrical isolation that can be achieved in ZnO and GaN [18, 19]. However, it has been proposed that the charge neutrality level (CNL) of $In_2O_3$ and CdO lies above the conduction band edge[20, 21], indicating a different defect evolution behavior. While this defect evolution have been investigated to some extent in SOs like ZnO and CdO [18, 20], less is known about other prominent SOs like $In_2O_3$ and $Ga_2O_3$. Hence, in order to fully control and utilize the advantages of SOs a profound knowledge of the intrinsic defect behavior is a prerequisite.

In SOs the cat-ion vacancies and oxygen interstitials tend to be acceptors, while the oxygen vacancies and cat-ion interstitials are donors[22] [23] [24]. To controllably introduce intrinisic defects, electron or ion irradiation can be utilized, where room temperature ion irradiation renderes ZnO highly resistive[18]. However, several of the primary defects tend to be highly mobile, where e.g. zinc interstitials in ZnO are mobile at room temperature with an activation energy for migration of $\sim 0.5$ eV[26]. This has been further substantiated by more recent defect studies showing the formation of a deep acceptor after low temperature irradiation and subsequent annealing around room temperature[27]. At sufficiently low temperatures, however, the ion induced primary intrinsic defects are frozen in and will

dominate the defect generation. This enables the study of primary defects and their influence on the electrical properties of the material. Moreover, low temperature irradiation combined with online electrical measurements enables to correlate intrinsic defects with the local charge neutrality level (CNL) [21].

Here we study the electrical conductivity of $In_2O_3$ and $Ga_2O_3$ after low temperature ion irradiation, where the sheet resistivity of $Ga_2O_3$ increase after bombardement of 1.5 MeV $C^+$ ions making irradiation a suitable tool for contact isolation. $In_2O_3$, on the other hand, show a more complex evolution of the resistivity with irradiation dose, where a reduced resistivity at higher dose indicate intrinsic donor generation in n-type $In_2O_3$ and a CNL within the conduction band.

## II. EXPERIMENTAL

The $In_2O_3$ samples were grown by pulsed laser deposition on (001)-oriented yttria-stabilized zirconia (YSZ) and r-plane saphire with a thickness of $\sim 450$ nm. The films where unintentionally doped with a room temperature (RT) carrier concentration $\sim 1.5 \times 10^{18}$ $cm^{-3}$. The $Ga_2O_3$ samples were grown on a MgO substrate to a thickness of $\sim 215$ nm, and had a carrier concentration of $4.8 \times 10^{17}$ $cm^{-3}$ at RT. All samples were $10 \times 10$ $mm^2$ in size. Ohmic contacts were deposited on the corners of the $In_2O_3$ grown on YSZ and the $Ga_2O_3$ samples using e-beam evaporation of 10 nm titanium (Ti) and 100 nm aluminum (Al), leaving an open area $\sim 6 \times 10$ $mm^2$ in the middle of the samples exposed to irradiation. The samples were then mounted via wirebonding to a closed-cycle helium cryostat connected to a 1 MV NEC Tandem accelerator. The samples were then cooled down and irradiated at a temperature of 35 K with either 1.5 MeV $C^+$ or 3.2 MeV $Si^+$ ions, having a projected range (Rp) of 1.3 and 1.5 $\mu$m, respectively, as estimated by Monte Carlo simulations using the SRIM code[28]. Hence, with film thicknesses $< 500$ nm, the implanted species themselves do not contribute to the electrical properties of the films. Consequtive irradiations were carried out with increasing dose or fluence (in the following the term dose will be used), ranging from $5 \times 10^{10}$ to $1.5 \times 10^{17}$ $cm^{-2}$, where the current voltage (IV) measurements were conducted online between each irradiation using a Keithley 6487 pico-ampermeter. The dose rate was increased from $1 \times 10^{10}$ to $1 \times 10^{13}$ $cm^{-2}s^{-1}$, with a maximum current density of $0.5\mu Acm^{-2}$.The temperature of the sample remained low for all doses except for the two

highest ones, where a slight increase up to $\sim$ 100 K was observed. After irradiation, the samples where heated to room temperature (RT) while measuring IV characteristics every 10 K. The sheet resistance of the film was calculated based on a region between 0.9 and 1.8 V from the IV curves in Fig. 1. The region was chosen to minimize effects of shifts in amplification setting in the amperemeter.

A rectifying junction of Mg doped $In_2O_3$ on r-plane sapphire were realized by deposition of p-type zinc cobalt oxide, and showed a rectification of more than 3 orders of magnitude between $\pm$1 V[29]. The heterojunction were wire bonded using 30 $\mu$m diameter gold wire to the measurement terminals, minimizing shadowing during implantation. The sample were loaded into the tandem accelerator described above, and cooled down and irradiated at a temperature of 35 K with 3.2 MeV $Si^+$ ions to a dose of $2.0 \times 10^{12}$ $cm^{-2}$[30]. After implantation, the sample were heated in the online chamber to a desired annealing temperature while undertaking either thermal admittance spectroscopy (TAS) or deep level transient spectroscopy (DLTS) measurements. TAS was conducted using an Agilent 4284A Precision LCR Meter (20 Hz - 1 MHz), while DLTS was performed using a 1 MHz Boonton 7200 capacitance meter, an Agilent 81104A 80 MHz pulse generator and a Lake-shore 332 temperature controller. A reverse bias of 0.8 V was applied with a filling pulse of 0.8 V and 50 ms duration for the DLTS measurements.

## III. RESULTS AND DISCUSSION

Figure 1 shows the IV characteristics of an $In_2O_3$ sample irradiated with 3.2 MeV $Si^{3+}$ ions with increasing dose. All IV curves show a linear relationship between the voltage and current, as expected from the Ohmic contacts. However, the slopes of the curves change, indicating a change in measured resistance. Since the contacts remain Ohmic, this increase is interpreted as an increase in the sheet resistance in the SO layer, i.e. a change in the carrier concentration and mobility in the $In_2O_3$ film. However, the change in slope do not follow the irradiation dose monotonically, indicating a non-linear relationship between sheet resistance and irradiation dose. Similar features were observed for $Ga_2O_3$ (not shown).

Figure 2 shows the sheet resistance as a function of irradiation dose for one $Ga_2O_3$ sample irradiated by 1.5 MeV $C^+$ ions and two $In_2O_3$ samples irradiated by 1.5 MeV $C^+$ or 3.2 MeV $Si^+$, respectively. In the sheet resistance profiles several regions have been identified, and

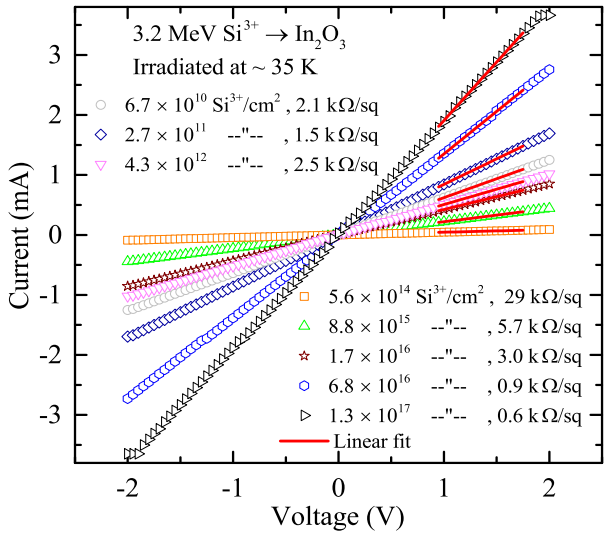


FIG. 1: Current-voltage characterization of an $In_2O_3$ sample subjected to 3.2 MeV $Si^{3+}$ irradiation with doses ranging from $5 \times 10^{10}$ to $1.3 \times 10^{17}$ $cm^{-2}$. Irradiation temperature was 35K with in situ IV characterization

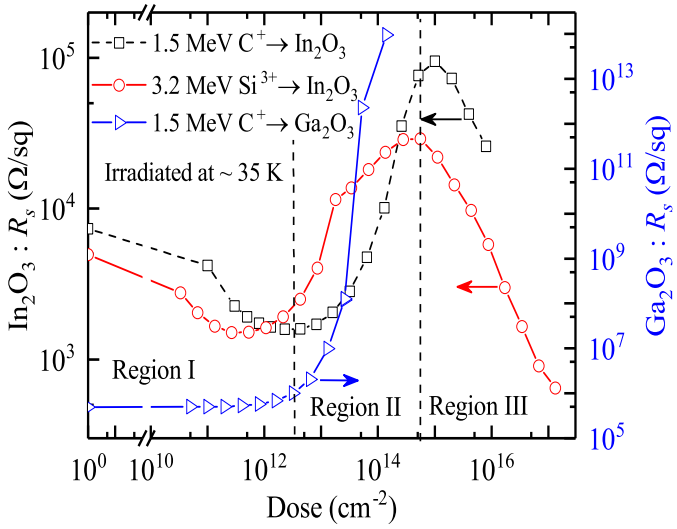


FIG. 2: Sheet resistance versus irradiation dose of 1.5 MeV $C^+$ and 3.2 MeV $Si^{3+}$ ions in $In_2O_3$ (left axis) and $Ga_2O_3$ (right axis) films

labelled region I-III. Starting with the $Ga_2O_3$ sample, $Ga_2O_3$ shows a close to unperturbed sheet resistance in region I, from $\sim 5 \times 10^5$ to $> 10^{13}$ Ohm/sq, before a monotonic increase occur above a dose of $\gtrsim 10^{13}$ $cm^{-2}$ (region II). For irradiation doses above $10^{14}$ $cm^{-2}$ , region III, the current is close to the detection limit of the electrometer. The monotonic increase in sheet resistance is similar to that observed in other semiconductors like ZnO

and GaN [18, 19] irradiated at room temperature, where H, Li, O and Si irradiations all showed increased resistance for doses above $10^{13}$ cm$^{-2}$. Hence, ion irradiation appears as a viable route to e.g. contact isolation in $Ga_2O_3$. Notice, however, that in contrast to the RT implantation by Kucheyev et al.[18] the present irradiations were carried out at 35 K , where migration and defect reactions of primary defects is expected to be negligible.

For $In_2O_3$, Fig. 2, a 1.5 MeV $C^+$ irradiation results in an initial small decrease in sheet resistance for low irradiation doses in region I, before it increases for doses between $10^{13}$ and $10^{15}$ cm$^{-2}$ in region II. However, when increasing the dose further, region III, the resistance peaks and decrease again. This is in strong contrast to that observed in $Ga_2O_3$ and ZnO. The results are further substantiated by a 3.2 MeV $Si^+$ irradiation, where similar features are observed, but where the sheet resistance profile is shifted towards lower doses due to the increased ion mass, and hence a stronger defect generation, of the Si ions compared to that of C.

From SRIM simulations, where the threshold energy for displacement of In atoms (and O atoms) was put to 15 eV, a typical value for semiconductors[31, 32], the vacancy generation from 1.5 MeV $C^+$ and 3.2 MeV $Si^{3+}$ ions is found to be 0.02 and 0.10 vacancies/ion/Ångstrom in the films. Thus, Si forms $\sim 5$ times more vacancies than C for the present conditions. Interestingly, the shift in resistivity as a function of dose between Si and C irradiated samples is also $\gtrsim 5$, although somewhat dose dependent, indicating a close to linear relationship between the ion mass and vacancy generation.

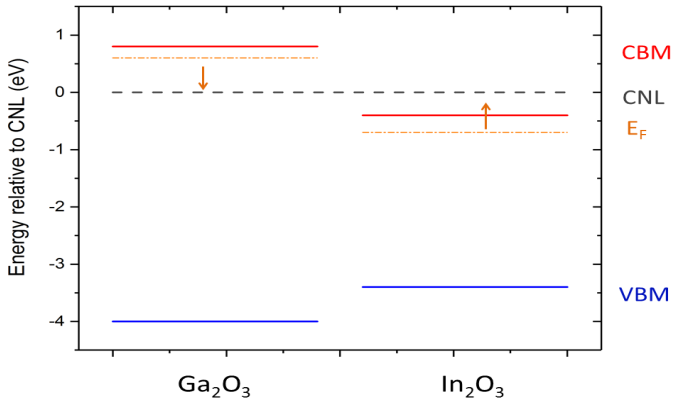


FIG. 3: A schematics of the charge neutrality level as predicted for $Ga_2O_3$ (left) and $In_2O_3$ with respect to VBM and CBM and the estimated Fermi level position before irradiation

Interestingly, the results in Fig. 2 are in accordance with the theory of a charge neutrality

level, as illustrated in Fig. 3. For $Ga_2O_3$ the CNL is estimated to be within the band gap, and hence the Fermi level is expected to move towards the midle of the band gap in the present samples resulting in a reduction in the resistivity, see Fig. 3. For $In_2O_3$, on the other hand, the CNL is proposed to be within the conduction band and the Fermi level is expected to more closer to CBM and an increased resistivity should occur after irradiation. Moreover, the reduction in the resistivity in $In_2O_3$ is in accordance with a surface accumulation layer and the fact that hydrogen is a donor [20]. For $Ga_2O_3$ a surface depletion layer is observed, but hydrogen is always a donor[24, 33]. However, this is a similar behavior to other SO's, like ZnO, where the CNL is within the band gap, while H is remains a donor[34].

After irradiation to the highest dose, the temperature was increased to room temperature while IV characteristics were measured every 10 K. Fig. 4 shows the calculated sheet resistance before and after irradiation, and after long term annealing at RT (9h). The sheet resistance of the $Ga_2O_3$ reduces from above $10^{15}$ Ohm/sq to around $10^{11}$ Ohm/sq. This is, however, still substantially higher than before irradiation. The reduction in sheet resistance may be due to thermal activation of charge carriers, or annealing of compensating defects. However, the main features of the ion induced resistance remains.

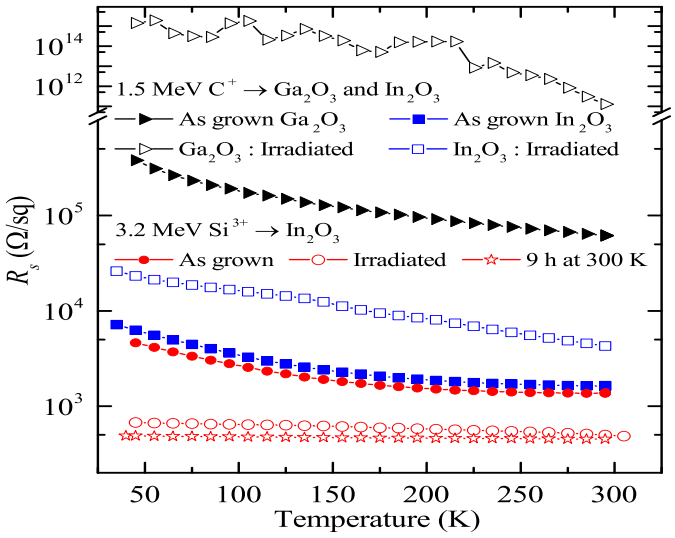


FIG. 4: Sheet resistance versus temperature for as grown $In_2O_3$ and after 1.5 MeV $C^+$ or 3.2 MeV $Si^{3+}$ irradiation at 35 K with a dose of $1 \times 10^{16}$ or $1.3 \times 10^{17}$ $cm^{-2}$, respectively. In addition, the sheet resistance after RT annealing for 9 hours is shown The The $Ga_2O_3$ sample was irradiated by 1.5 MeV $C^+$ with a dose of $1 \times 10^{14}$ $cm^{-2}$.

A reduction in sheet resistivity with increased temperature is also seen for the $In_2O_3$

samples after irradiation. Moreover, after annealing at RT for 9 hours an additional temperature scan of the resistance was performed, Fig. 4, and shows that the sheet resistance has decreased even further. The results indicate an asymmetric formation of dopants, where more donor-like than acceptor-like defects are formed and stable at RT, in strong contrast to that of $Ga_2O_3$.

To gain further insight into the defect formation in the $In_2O_3$, irradiation was performed on a heterojunction using 3.2 MeV $Si^{3+}$ ions to a dose of $2 \times 10^{12}$ cm$^{-2}$. Fig. 5(a) shows thermal admittance measurements for the heterojunction before and after irradiation[2]. Before irradiation, two steps in the capacitance are observed, indicating two shallow levels in the as grown material, and estimated to have activation energies of 20 meV and 180 meV below the conduction band edge ($E_C$). After irradiation, the capacitance increases somewhat, where the red line is after an anneal at 110K, supporting the indication of an increase in charge carrier concentration for irradiation doses up to $\sim 10 \times 10^{13}$ cm$^{-2}$. During the increase from irradiation temperature to RT (Fig. 5(a)), the capacitance of the contact decreases slightly, indicating a loss in charge carriers. However, the shallow level at $E_C - 0.02$ eV remains as the dominant donor level, and no new shallow defect levels are observed.

Figure 5(b) shows DLTS spectra before and after irradiation. At least two deep level defects are observed in the upper part of the band gap, with activation energies of 0.26[29] and 0.31 eV[2] below $E_C$. After irradiation, the DLTS signature is qualitatively the same, but with a small reduction in the DLTS amplitude. However, the charge carrier concentration has increased, leaving the overall trap concentration similar to the as grown state. Hence, there is no significant change in the deep level defects as observed by DLTS. Interestingly, the oxygen vacancy ($V_O$ ) is expected to be a deep donor in the bulk of $In_2O_3$, but none of the observed deep level defects show a response proportional to the irradiation dose, even at this relatively high dose. However, note that the irradiation is in the low dose regime, since the heterojunction would not remain rectifying for doses above $10^{14}$ cm$^{-2}$ Interestingly, the reduction in resistivity in In2O3 after irradiation is in line with that predicted by the CNL (Fig. 6(b)), the surface accumulation layer and the fact that hydrogen is a donor[20]. However, while the CNL for $Ga_2O_3$ is expected to be within the band gap and a surface depletion is observed, hydrogen is still always a donor. .

The primary defects in $Ga_2O_3$ and $In_2O_3$ are expected to have similar charge state behavior, as shown by first principles calculation, and schematically shown in Fig. 6(a) based

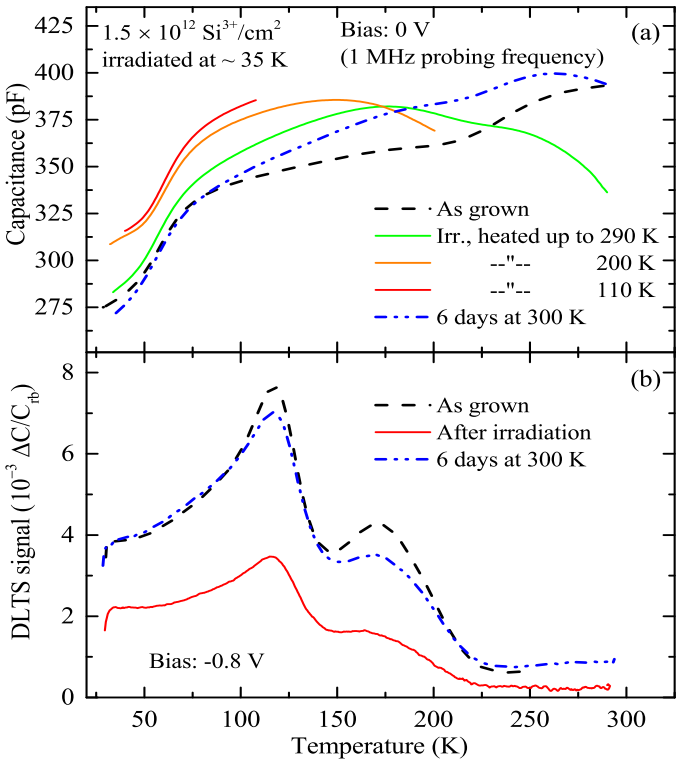


FIG. 5: Capacitance versus temperature (a) and DLTS spectra of an $In_2O_3$ based heterojunction before and after a 3.2 MeV $Si^3+$ irradiation at 35 K.

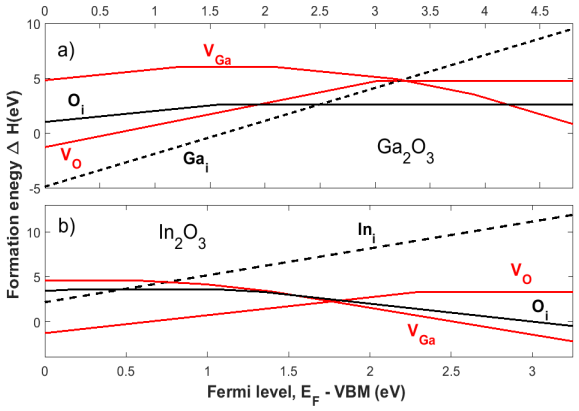


FIG. 6: A schematic representation of the formation energies of primary defects in (a) $In_2O_3$ and (b) $Ga_2O_3$, where vacancies and interstitials are marked in red and black, respectively. The schematic is based on the work of [23] and [25]

on the work by Lany and Zunger[23] and Deak et al.[25]. For a Fermi level close to the conduction band edge, the gallium vacancy in $Ga_2O_3$ and the indium vacancy ($V_{In}$ ) in $In_2O_3$ are expected to be in the -3 charge state, the oxygen interstitial ($O_i$) in -2 for $In_2O_3$

and neutral in $Ga_2O_3$, and the indium and gallium interstitials ($In_i$ and $Ga_i$ in $In_2O_3$ and $Ga_2O_3$, respectively) in the +3 charge states. The $V_O$, on the other hand, is expected to be a deep donor, and will be neutral in highly n-type material. Assuming that only isolated primary point defects are being generated and the theoretical considerations hold, $Ga_2O_3$ should remain charge neutral after irradiation, while an increase in sheet resistivity due to the formation of more ionized acceptors compared to donors due to the neutral oxygen vacancy. Therefore, an explanation based on primary defects alone (Fig. 6(a)) do not hold. Interestingly, this increase occurs at a slightly lower dose for the $Ga_2O_3$ sample compared to that of $In_2O_3$, indicating less dynamic annealing occuring in $Ga_2O_3$. However, at doses above $10^{14}$ cm$^{-2}$ the sheet resistivity of $Ga_2O_3$ and $In_2O_3$ deviate, where a model based on primary defects alone for the change in sheet resistivity is insufficient.

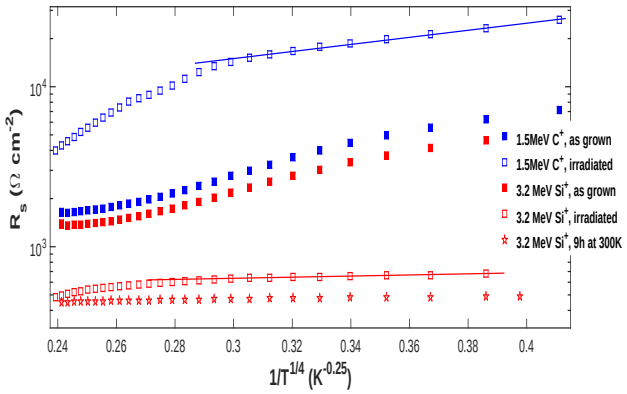


FIG. 7: Sheet resistance versus temperature$^{1/4}$ for as grown $In_2O_3$ and after 1.5 MeV $C^+$ or 3.2 MeV $Si^{3+}$ irradiation at 35 K with a dose of $1 \times 10^{16}$ or $1.3 \times 10^{17}$ cm$^{-2}$, respectively.

Assuming that only a few percent survive after the dynamic annealing, a dose of $10^{14}$ cm$^{-2}$ corresponds to a vacancy generation in the order of $\sim 10^{19}$ cm$^{-3}$, i.e. an average distance of $\sim 5$ nm between each vacancy. Hence for irradiation doses above $10^{15}$ cm$^{-2}$ the distance between the defects are low. It has previously been proposed that the electrical conduction in disordered layers from ion irradiation can occur via tunnel-assisted hopping between disordered states[35–38]. In a low temperature range where there are few phonons and carriers jump between states with small energy differences but longer distances, the conductivity behaves as $\Omega \propto T^{-1/4}$. At higher temperatures, however, carriers may move between near states by phonon assistant hopping, and a $T^{-1}$ dependence is expected. Figure 7 shows the the sheet restistance versus $T^{-1/4}$. Indeed, a close to linear region is observed

for the sheet resistance up to $\sim$ 120 K for the irradiated samples (indicated by the solid line in Fig. 4(b) ), in contrast to before irradiation, indicating that a hopping mechanism may be the origin of the reduced resistivity for the high dose irradiations. However, the variation in sheet resistance is significantly lower than that reported in, e.g. GaAs [35], and although a $T^{-1/4}$ shows the best fit within a region in the low temperature range, other models cannot be excluded.

On the other hand, at high irradiation doses the assumption of generating isolated point defect may no longer hold, i.e. in Region III (Fig. 2), and larger intrinsic defect clusters may arise, as observed in e.g. ZnO using rutherford backscattering spectrometry [39] potentially also involving impurities. While charge neutrality may be maintained between the vacancies and interstitials for individual Frenkel pairs, larger agglomerates may favor either donor or acceptor like defects. Hence, two explanations for the observed resistivity behavior in $In_2O_3$ is i) electrical conduction via tunnel-assisted hopping between disordered states, or ii) larger defect complexes are donor like, in contrast to that of $Ga_2O_3$ where the dominant defect generation compensate the n-type conductivity. This may bridge the microscopic defect generation to CNL, where the CNL in $In_2O_3$ is expected to be within the conduction band, in contrast to that of $Ga_2O_3$ where the CNL is found inside the band gap.

## IV. CONCLUSIONS

In summary, we have studied the evolution of sheet resistance of n-type $In_2O_3$ and $Ga_2O_3$ exposed to bombardment with MeV $^{12}C$ and $^{28}Si$ ions at low temperature. The sheet resistance of $Ga_2O_3$ increased by more tha 8 orders of magnitude as a result of ion irradiation, in line with that observed in other semiconducting oxides like ZnO. $In_2O_3$, on the other hand, became more conductive when irradiated at doses above $\sim 10^{15}$ cm$^{-2}$. Thermal admittance spectroscopy and deep level transient spectroscopy did not reveal new defect levels for irradiation up to $2 \times 10^{12}$ cm$^{-2}$. A model where larger defect complexes preferentially produce donor like defects in $In_2O_3$ is proposed, and may reveal a microscopic view of a charge neutrality level within the conduction band, as previously proposed.

**Acknowledgments**

Financial support is acknowledged from the Research Council of Norway through the FriPro program (Project No. 239895), and the Deutsche Forschungsgemeinschaft

---

[1] R.B.H. Tahar, T. Ban, Y. Ohya, and Y. Takahashi, J. Appl. Phys. **83**, 2631 (1998).

[2] H. von Wenckstern, D. Splith, F. Schmidt, M. Grundmann, O. Bierwagen, and J.S. Speck, APL Mater. **2**, 046104 (2014).

[3] Y. Kokubun, K. Miura, F. Endo, and S. Nakagomi, Appl. Phys. Lett. **90**, 031912 (2007).

[4] M. Higashiwaki, K. Sasaki, H. Murakami, Y. Kumagai, A. Koukitu, A. Kuramata, T. Masui, and S. Yamakoshi, Semicond. Sci. Technol. **31**, 034001 (2016).

[5] A. Baldereschi and E. Tosatti, Phys Rev. B **17**, 4710 (1978).

[6] E. Tokumitsu, Jpn. J. Appl. Phys. **29**, L698 (1990).

[7] W. Walukiewicz, Phys Rev. B **37**, 4760 (1988).

[8] A. Zunger, Appl. Phys. Lett. **83**, 57 (2003).

[9] W. Monch, Appl. Phys. Lett. **86**, 162101 (2005).

[10] J. Tersoff and W. A. Harrison, Phys. Rev. Lett. **58**, 2367 (1987).

[11] C.G. Van de Walle and J. Neugebauer, Nature **423**, 626 (2003).

[12] A. Klein, Thin Solid Films **520**, 3721 (2012).

[13] J. Robertson, Microelectronic Engineering **86**, 1558 (2009).

[14] B. Hoffling, A. Schleife, C. Rodl, and F. Bechstedt, Phys Rev. B **85**, 035305 (2012).

[15] A. Schleife, F. Fuchs, C. Rodl, J. Furthmuller, and F. Bechstedt, Appl. Phys. Lett. **94**, 012104 (2009).

[16] J. Robertson, K. Xiong, and S.J. Clark, Thin Solid Films **496**, 1 (2006).

[17] J. Robertson and B. Falabretti, J. Appl. Phys. **100**, 014111 (2006).

[18] S. O. Kucheyev, P.N.K. Deenapanray, C. Jagadish, J. S. Williams, M. Yano, K. Koike, S. Sasa, M. Inoue,and K. Ogata, Appl. Phys. Lett. **81**, 3350 (2002).

[19] H. Boudinov, S.O. Kucheyev, J. S. Williams, C. Jagadish, and G. Li, Appl. Phys. Lett. **78**, 943 (2001).

[20] P. D. C. King, T. D. Veal, D. J. Payne, A. Bourlange, R.G. Egdell, and C. F. McConville,

Phys. Rev. Lett. **101**, 116808 (2008).

[21] P. D. C. King, T. D. Veal, P. H. Jefferson, J. Zuniga-Perez, V. Munoz-Sanjose, C. F. McConville, Phys. Rev. B **79**, 035203 (2009).

[22] A. Janotti and C. G. Van de Walle, Rep. Prog. Phys. **72**, 126501 (2009).

[23] S. Lany and A. Zunger, Phys. Rev. Lett. **98**, 045501 (2007).

[24] J. B. Varley, J. R. Weber, A. Janotti, and C. G. Van de Walle, Appl. Phys. Lett. **97**, 142106 (2010).

[25] P. Deak, Q.D. Ho, F. Seemann, B. Aradi, M. Lorke, and T. Frauenheim, Phys. Rev. B **95**, 075208 (2017).

[26] A. Janotti and C. G. Van de Walle, Phys. Rev. B **76**, 165202 (2007).

[27] C. Bhoodoo, A. Hupfer, L. Vines, E. V. Monakhov, and B. G. Svensson, Phys. Rev. B, **94**, 205204 (2016).

[28] J.F. Ziegler, J.P. Biersack, and U. Littmark, *The stopping and Range of Ions in Solids* (Pergamon, New York, 1985).

[29] H.von Wenckstern, D. Splith, S. Lanzinger, F. Schmidt, S. Müller, P. Schlupp, R. Karsthof, and M. Grundmann, Adv. Elec. Mater. **1**, 1400026 (2015).

[30] A higher irradiation dose results in a loss of rectifying behavior and the structure will no longer be suitable for TAS and DLTS.

[31] J. J. Loferski and P. Rappaport, Phys. Rev. **111**, 432 (1958).

[32] B. G. Svensson, C. Jagadish, A. Hallén, and J. Lalita, Phys. Rev. B. **55**, 10498 (1997).

[33] P.D.C. King, I. McKenzie, and T.D. Veal, Appl. Phys. Lett. **96**, 062110 (2010).

[34] C.G. Van de Walle, Phys. Rev. Lett. **85**, 1012 (2000).

[35] Y. Kato, T. Shimada, Y. Shiraki, and K. F. Komatsubara, J. of Appl. Phys. **45**, 1044 (1974).

[36] N. F. Mott, J. Non-Cryst. Solids **1**, 1 (1968).

[37] N.F. Mott, Philos. Mag. **19**, 835 (1969).

[38] M.H. Cohen, H. Fritzsche, and S. R. Ovshinsky, Phys. Rev. Lett. **22**, 1065 (1969).

[39] E. Wendler, W. Wesch, A. Yu. Azarov, N. Catarino, A. Redondo-Cubero, E. Alves, and K. Lorenz, Nucl. Instr. Met. Phys. Res. B. **307**, 394 (2013).